Available online at www.sciencedirect.com
ScienceDirect
International Journal of Thermal Sciences 48 (2009) 691–698
International Journal of Thermal Sciences
www.elsevier.com/locate/ijts

Chebyshev collocation spectral method for one-dimensional radiative heat transfer in graded index media

Ya-Song Sun, Ben-Wen Li *

Key Laboratory of National Education Ministry for Electromagnetic Processing of Materials, P.O. Box 314, Northeastern University, Shenyang 110004, China

Received 30 March 2008; received in revised form 24 June 2008; accepted 7 July 2008

Available online 31 July 2008

Abstract

Chebyshev spectral collocation method based on discrete ordinates equation is developed to solve radiative transfer problems in a one-dimensional absorbing, emitting and scattering semitransparent slab with spatially variable refractive index. For radiative transfer equation, the angular domain is discretized by discrete ordinates method, and the spatial domain is discretized by Chebyshev collocation spectral method. Due to the exponential convergence of spectral methods, a very high accuracy can be obtained even using few nodes for present problems. Numerical results by the Chebyshev collocation spectral-discrete ordinates method (SP-DOM) are compared with those available data in references. Effects of refractive index gradient on radiative intensity are studied for space dependent scattering media. The results show that SP-DOM has a good accuracy and efficiency for solving radiative heat transfer problems in even spatially varying absorbing, emitting, scattering, and graded index media.

Keywords: Radiative heat transfer; Graded index; Semitransparent media; Chebyshev collocation spectral methods

1. Introduction

In graded index media, the ray goes along a curved path determined by the Fermat principle. As a result, the solution of radiative transfer in graded index media is more difficult than that in uniform index media. The radiative heat transfer in a semitransparent media with a graded index has evoked wide interest of many researchers. In the early 1993, Siegel and Spuckler [1] have developed a model of one-dimensional composite media made of several sublayers, each of them being treated as a slab at uniform index bounded by diffuse surfaces. Ben Abdallah and Le Dez [2,3] presented a curved ray tracing technique to analyze the radiative heat transfer in semitransparent media with a graded index. Huang et al. [4] proposed a ray splitting and tracing method to solve the problem of radiative heat transfer in graded index media. For the radiative transfer problems in one-dimensional semitransparent media with spatially variable refractive index, Liu et al. [5] proposed a Monte Carlo curved ray-tracing technique, Huang et al. developed a combined curved ray-tracing and pseudo-source adding method [6], and a discrete ray-tracing method [7–10]. Recently, Tan et al. [11] proposed the discrete ray-tracing method to solve transient coupled heat transfer in semitransparent media with graded refractive index. Huang et al. [12] proposed a backward ray tracing method and a backward Monte Carlo method to solve heat transfer in two-dimensional semitransparent medium with graded refractive index. The discrete ordinates method (DOM) for the radiative transfer equation (RTE) for a slab with variable refractive index is presented by Lemonnier and Le Dez [13]. Other methods for this kind of problems are finite element method (FEM) [14], finite volume method (FVM) [15], meshless local Petrov–Galerkin method (MLPG) [16], and least squares spectral element method (LSSEM) [17].

In the field of numerical simulations, it is well known that the FEM and the FVM can provide linear convergence, while, the spectral methods can provide exponential convergence [18]. Spectral methods have been widely applied in computational fluid dynamics [19,20], electrodynamics [21] and magnetohydrodynamics [22,23]. Despite the high accuracy and efficiency

* Corresponding author. Tel.: +86 24 83681756; fax: +86 24 83681758.
E-mail addresses: heatli@hotmail.com, heatli@epm.neu.edu.cn (B.-W. Li).

1290-0729/$ – see front matter
doi:10.1016/j.ijthermalsci.2008.07.003

of spectral methods, they are seldom applications of spectral methods in radiative heat transfer computation. Recently, for radiative and conductive heat transfer in a concentric spherical and cylindrical media with a uniform index, Aouled–Dlala et al. [24] proposed a finite Chebyshev transform (FCT) to treat the angular derivative terms in cylindrical and spherical systems. Li et al. [25] have developed the Chebyshev collocation spectral method for one-dimensional radiative heat transfer even with anisotropic space dependent scattering medium with a uniform index.

In this paper, we extend the collocation spectral method to solve the radiative transfer problem in a one-dimensional semi-transparent slab with a graded index based on discrete-ordinates equation. In the following of this paper, the physical model and governing equation will be presented in the second section. The SP-DOM formulations for radiative transfer equation for graded index media and the solution procedure will be presented in detail in the third section. Validations by typical cases with available numerical results and the discussion of effects of the refractive index gradient on radiative intensity are made in the fourth section. Finally, the last section gives the conclusions.

2. Physical model and governing equation

We consider one-dimensional semitransparent gray absorbing, emitting and scattering slab with thickness L bounded by two opaque, diffuse and gray walls (see Fig. 1). The refractive index $n(x)$ varies along the axis coordinate x. The absorption coefficient and scattering coefficient are k_a and k_s. On both sides of the slab, the emissivities are ε_0 and ε_L, and the temperatures are assumed to be T_0 and T_L, respectively.

The governing equation for radiative transfer in one-dimensional absorbing, emitting, and scattering media with graded index in term of radiation intensity reads [13]

$$n^2\frac{d}{ds}\left(\frac{I(x,\mu)}{n^2}\right)+(k_a+k_s)I(x,\mu) = n^2k_aI_b(x)+\frac{k_s}{2}\int_{-1}^{1}I(x,\mu')\Phi(\mu',\mu)\,d\mu' \quad \text{in } [0,L]\times[-1,1] \tag{1}$$

with boundary conditions:

$$I(0,\mu)=\varepsilon_0 n_0^2\frac{\sigma T_0^4}{\pi}+2(1-\varepsilon_0)\int_{-1}^{0}I(0,\mu')|\mu'|\,d\mu' \quad \text{on } x=0,\quad \mu\in(0,1] \tag{2a}$$

$$I(L,\mu)=\varepsilon_L n_L^2\frac{\sigma T_L^4}{\pi}+2(1-\varepsilon_L)\int_{0}^{1}I(L,\mu')|\mu'|\,d\mu' \quad \text{on } x=L,\quad \mu\in[-1,0) \tag{2b}$$

where s is the curvilinear abscissa along a (curved) path, $I(x,\mu)$ is the radiation intensity at position x and direction cosine μ, $I_b(x)$ is the blackbody radiation intensity at the temperature of the media $T(x)$, $\Phi(\mu',\mu)$ is the scattering phase function of energy transfer from an incoming direction cosine μ' to an outgoing direction cosine μ, and σ is Stefan–Boltzmann constant.

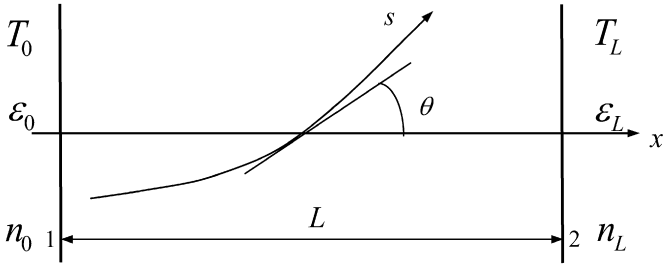

Fig. 1. Physical geometry of slab.

In the one-dimensional Cartesian coordinate system, the conservative form of radiative transfer equation within graded index media can be rewritten as [13]

$$\mu\frac{\partial I(x,\mu)}{\partial x}+\gamma\left(1-\mu^2\right)\frac{\partial I(x,\mu)}{\partial\mu}+(k_a+k_s-2\gamma\mu)I(x,\mu) = n^2k_aI_b+\frac{k_s}{2}\int_{-1}^{1}I(x,\mu')\Phi(\mu',\mu)\,d\mu' \tag{3}$$

where γ is the derivative of refractive index after natural logarithm with respect to the coordinate x

$$\gamma=\frac{d(\ln n)}{dx} \tag{4}$$

The boundary condition expressions for Eq. (3) take the same form as Eq. (2).

3. Discretization of RTE for graded index media and the solution procedure

3.1. Discrete-ordinates equation of radiative transfer equation for graded index media

The one-dimensional DOM form of Eq. (3) reads

$$\mu^m\frac{\partial I^m(x)}{\partial x}+\gamma\left\{\frac{\partial}{\partial\mu}\left[\left(1-\mu^2\right)I(x)\right]\right\}_{\mu=\mu^m}+(k_a+k_s)I^m(x) = n^2k_aI_b(x)+\frac{k_s}{2}\sum_{m'=1}^{M}I^{m'}(x)\Phi\left(\mu^{m'},\mu^m\right)w_{m'} \quad m=1,2,\ldots,M \tag{5}$$

with boundary conditions

$$I_0^m=\frac{\varepsilon_0 n_0^2\sigma T_0^4}{\pi}+2(1-\varepsilon_0)\sum_{\mu^{m'}<0}I_0^{m'}|\mu^{m'}|w^{m'} \quad \mu^m>0 \tag{6a}$$

$$I_L^m=\frac{\varepsilon_L n_L^2\sigma T_L^4}{\pi}+2(1-\varepsilon_L)\sum_{\mu^{m'}>0}I_L^{m'}|\mu^{m'}|w^{m'} \quad \mu^m<0 \tag{6b}$$

The angular derivative term in Eq. (5) is discretized by central difference scheme, and its final form can be written as [26]

$$\left\{\frac{\partial}{\partial\mu}\left[\left(1-\mu^2\right)I(x)\right]\right\}_{\mu=\mu^m} \approx \frac{\alpha^{m+1/2}I^{m+1/2}-\alpha^{m-1/2}I^{m-1/2}}{w^m} \tag{7}$$

Here, $I^{m+1/2}$ and $I^{m-1/2}$ are the angular intensities in the directions $m+1/2$ and $m-1/2$, and the central difference scheme is adopted to correlate them to the unknown I^m, i.e., $I^m=\frac{1}{2}(I^{m+1/2}+I^{m-1/2})$. The constants $\alpha^{m\pm1/2}$ only depend on the difference scheme and can be determined by the following recurrences

$$\alpha^{1/2}=\alpha^{M+1/2}=0 \tag{8a}$$

$$\alpha^{m+1/2}-\alpha^{m-1/2}=-2w^m\mu^m \tag{8b}$$

Now, Eq. (5) can be rewritten as

$$\begin{aligned}\mu^m\frac{\partial I^m}{\partial x}&+\left[\frac{1}{w^m}\max(\gamma\alpha^{m+1/2},0)+\frac{1}{w^m}\max(-\gamma\alpha^{m-1/2},0)\right.\\&\left.+\left(k_a+k_s-\frac{k_s}{2}\Phi^{m,m}w_m\right)\right]I^m\\&=\frac{1}{w^m}\left[\max(-\gamma\alpha^{m+1/2},0)I^{m+1}+\max(\gamma\alpha^{m-1/2},0)I^{m-1}\right]\\&\quad+k_an^2\sigma T^4/\pi+\frac{k_s}{2}\sum_{m'=1,m'\neq m}^{M}I^{m'}(x)\Phi^{m',m}w_{m'}\end{aligned} \tag{9}$$

where T is the absolute temperature distribution within the media, and is determined by

$$T(x)=\left[\frac{\pi}{2\sigma n^2(x)}\sum_{m=1}^{M}I^m(x)w_m\right]^{1/4} \tag{10}$$

In angular domain, the S_N approximation has been chosen. The ordinate direction cosine μ^m and quadratic weighing factor w^m are given in Ref. [27].

3.2. Chebyshev collocation spectral formulations

The Chebyshev–Guass–Lobatto collocation points [19,20,28] are used for spatial discretization

$$s_j=\cos\frac{\pi j}{N},\quad j=0,1,\ldots,N \tag{11}$$

Then, the mapping of arbitrary interval $[X_1,X_2]$ to standard interval $[-1,1]$ is needed to fit the requirement of Chebyshev polynomial

$$s=\frac{2x-(X_2+X_1)}{(X_2-X_1)},\qquad x=\frac{s(X_2-X_1)+X_2+X_1}{2} \tag{12}$$

After mapping Eq. (9) becomes

$$\begin{aligned}\mu^m\left(\frac{2}{X_2-X_1}\right)\frac{\partial I^m(s)}{\partial x}&+\left[\frac{1}{w^m}\max\left(\gamma\alpha^{m+1/2},0\right)\right.\\&\left.+\frac{1}{w^m}\max\left(-\gamma\alpha^{m-1/2},0\right)\right.\\&\left.+\left(k_a+k_s-\frac{k_s}{2}\Phi^{m,m}w_m\right)\right]I^m(s)\\&=\frac{1}{w^m}\left[\max\left(-\gamma\alpha^{m+1/2},0\right)I^{m+1}(s)\right.\\&\left.+\max\left(\gamma\alpha^{m-1/2},0\right)I^{m-1}(s)\right]\\&\quad+k_an^2\sigma T^4/\pi+\frac{k_s}{2}\sum_{m'=1,m'\neq m}^{M}I^{m'}(s)\Phi^{m',m}w_{m'}\end{aligned} \tag{13}$$

The radiative intensity can be approximated by

$$I_N^m(s)=\sum_{k=0}^{N}\hat{I}_k^mT_k(s) \tag{14}$$

where $I_N^m(s)\approx I^m(s)$, the coefficients $\hat{I}_k^m$ are determined by the collocation points s_k, $k=0,1,\ldots,N$; and the $T_k(s)$ is the first kind Chebyshev polynomial. The polynomial of degree N defined by Eq. (14) can be the Lagrange interpolation polynomial based on the set $\{s_i\}$ like

$$I_N^m(s)=\sum_{j=0}^{N}h_j(s)I^m(s_j) \tag{15}$$

where $h_j(s)$ is a function of the first order derivative of Chebyshev polynomial, and its detail definition and expression can be found in Ref. [20].

To avoid spectral coefficients solution and fast cosine transformation, we use Eq. (15) rather than Eq. (14) in Eq. (13).

3.3. Discretization and numerical implementation

Substituting Eq. (15) into Eq. (13), one can obtain the spectral discretized linear equations

$$\left(\mathbf{A}^m+\mathbf{B}^m\right)\mathbf{I}^m=\mathbf{F}^m,\quad m=1,2,\ldots,M \tag{16}$$

where the elemental expressions for matrix $\mathbf{A}^m$, $\mathbf{B}^m$, and $\mathbf{F}^m$ are

$$A_{ik}^m=\mu^m\left(\frac{2}{X_2-X_1}\right)D_{s,ik}^{(1)} \tag{17a}$$

$$B_{ik}^m=\begin{cases}\dfrac{1}{w^m}\left(\max\left(\gamma(s_i)\alpha^{m+1/2},0\right)\right.\\\quad\left.+\max\left(-\gamma(s_i)\alpha^{m-1/2},0\right)\right)\\\quad+\left(k_a+k_s-\dfrac{k_s}{2}\Phi^{m,m}w_m\right), & i=k\\0, & \text{otherwise}\end{cases} \tag{17b}$$

$$\begin{aligned}f_i^m=&\frac{1}{w^m}\left[\max\left(-\gamma(s_i)\alpha^{m+1/2},0\right)I^{m+1}(s_i)\right.\\&\left.+\max\left(\gamma(s_i)\alpha^{m-1/2},0\right)I^{m-1}(s_i)\right]\\&+k_an^2\sigma T^4(s_i)/\pi+\frac{k_s}{2}\sum_{m'=1,m'\neq m}^{M}I^{m'}(s_i)\Phi^{m,m'}w_{m'}\end{aligned} \tag{17c}$$

and the matrix $\mathbf{D}_s^{(1)}$ is the first order derivative matrix in s direction corresponding to Chebyshev–Lobatto–Lobatto collocation points [19,20,28].

Boundary conditions, given by Eqs. (6a) and (6b), must be imported before solving Eq. (16). For the Dirichlet boundary

condition, it can be easily imported and the detail can be found in Refs. [18–20,28].

The implementation of Chebyshev collocation spectral method can be carried out according to the following routine:

Step 1: Choose the number of nodes N_{node} and compute the coordinate values of nodes, hence to compute the derivative of refractive index $\gamma(s)$ at nodes.

Step 2: Choose the direction number M and the corresponding direction cosine, as well as the weights w_m, hence to compute the angular difference constants α.

Step 3: Give radiative intensity an initial assumption (zero, for example) in all directions except for boundary condition, and assemble to get the matrix $\mathbf{F}^m$ by Eq. (17c).

Step 4: Start iteration in each angular direction for $m = 1, 2, \ldots, M$, and assemble to get matrix $\mathbf{A}^m$, $\mathbf{B}^m$, and $\mathbf{F}^m$ by Eqs. (17a)–(17c).

Step 5: Compute the boundary radiative intensities according to Eqs. (6a) and (6b) and import the boundary conditions by Eq. (17c).

Step 6: Directly solve Eq. (16) by $\mathbf{I}^m = (\mathbf{A}^m + \mathbf{B}^m)^{-1}\mathbf{F}^m$.

Step 7: Terminate the iteration if the relative maximum absolute difference of radiative intensities, say, $\max\{|(\mathbf{I}^m)^{\text{new}} - (\mathbf{I}^m)^{\text{old}}|/(\mathbf{I}^m)^{\text{old}}\}$ for all nodes and directions, is less than the tolerance (10^{-8} in our work, for example), otherwise, go back to Step 4.

4. Numerical results and discussions

In the field of numerical simulations, the main superiorities of spectral methods over others like FEM, FVM, and finite difference method (FDM), are exponential convergence and high accuracy [18].

In our present work, the numerical results are presented for radiation in a graded index. For the purpose of comparison with the SP-DOM solutions, various test cases are selected because very precise solutions of the radiative transfer equation exist. All the computations are executed on a computer with CPU of Pentium(R) D (3.40 GHz) and 1.49 GB RAM.

4.1. Example 1: Radiative equilibrium in non-scattering media with linear refractive index

The SP-DOM is applied to a one-dimensional slab bounded by black walls. As shown in Fig. 1, the temperatures of boundary walls are assumed to be $T_0 = 1000$ K and $T_L = 1500$ K, respectively. The absorption coefficient k_a and scattering coefficient k_s are uniform through the slab. The refractive index of the media within the slab varies linearly with the axis coordinate and can be expressed as $n(x) = 1.2 + 0.6x/L$. The media within the slab is non-scattering. This case has also been adopted as a test one by Huang et al. [6] for the pseudo source adding method validation and Liu [14] for the finite element method validation.

The temperature distributions by SP-DOM within the media are plotted in Fig. 2 for three values of slab optical thicknesses, namely, $\tau_L = 0.01$, $\tau_L = 1.0$, and $\tau_L = 3.0$, respectively. Here

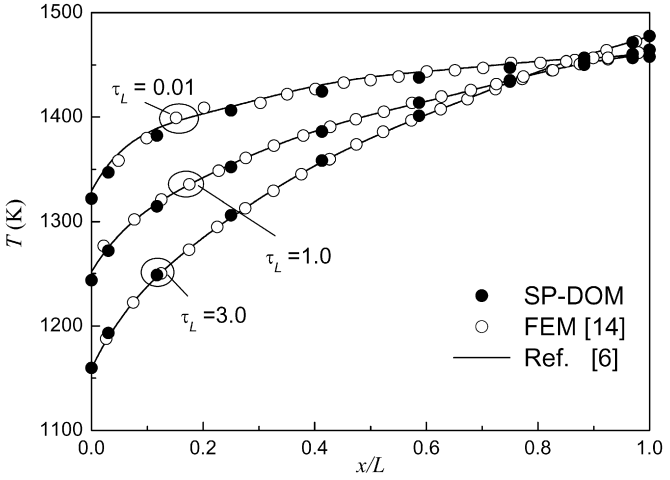

Fig. 2. Temperature distributions in the case of $n(x) = 1.2+0.6x/L$, $\varepsilon_0 = \varepsilon_L = 1.0$.

Table 1
The dimensionless radiative heat fluxes on different nodes in the case of $n(x) = 1.2 + 0.6x/L$ and $\varepsilon_0 = \varepsilon_L = 1.0$

x/L	$\psi = 2\pi \int_{-1}^{1} I\mu\, d\mu/[n_0^2\sigma(T_0^4 - T_L^4)]$		
	$\tau_L = 0.01$	$\tau_L = 1.0$	$\tau_L = 3.0$
0.00000	0.99655	0.70860	0.42303
0.03015	0.99655	0.70863	0.42306
0.11698	0.99655	0.70860	0.42303
0.25000	0.99655	0.70863	0.42306
0.41318	0.99655	0.70860	0.42303
0.58682	0.99655	0.70863	0.42306
0.75000	0.99655	0.70860	0.42303
0.88302	0.99655	0.70863	0.42306
0.96985	0.99655	0.70860	0.42303
1.00000	0.99655	0.70863	0.42306

the number of nodes $N_{\text{node}} = 9$ is used for spatial discretization, and the total solid angle is subdivided into $M = 8$. The CPU time are 0.1736, 0.5502, 1.2540 s for $\tau_L = 0.01$, $\tau_L = 1.0$, and $\tau_L = 3.0$, respectively. As shown in Fig. 2, the SP-DOM results are in good agreement with the results obtained by using the pseudo source adding method and FEM. Compared with the results from FEM, the maximum relative error is less than 0.68%.

The SP-DOM approximation of the dimensionless radiative heat fluxes based on different nodes within the slab with $n(x) = 1.2 + 0.6x/L$ and $\varepsilon_0 = \varepsilon_L = 1.0$ are listed in Table 1.

The dimensionless radiative heat fluxes are defined by

$$\psi = \left[2\pi \int_{-1}^{1} I\mu\, d\mu\right] \Big/ \left[n_0^2\sigma\left(T_0^4 - T_L^4\right)\right] \tag{18}$$

Theoretically, the dimensionless radiative heat fluxes for each node should keep the same value; however, results on different nodes obtained by numerical methods usually oscillate around the averaged value. The averaged dimensionless radiative heat fluxes for three optical thicknesses of $\tau_L = 0.01$, $\tau_L = 1.0$, and $\tau_L = 3.0$ by SP-DOM are $\psi_{\text{av}} = 0.99655$, $\psi_{\text{av}} =$

Table 2
The averaged dimensionless radiative heat fluxes in the case of blackbody boundaries and linear refractive index

n_0	n_L	τ_L	ψ_{av}		
			RT [13]	MLPG [16]	SP-DOM
1.0	1.5	0.1	0.96960	0.97040	0.96570
1.0	1.5	1.0	0.72430	0.72410	0.70870
1.0	1.5	10.0	0.17270	0.17440	0.17120
1.0	3.0	0.1	0.98720	0.99470	0.98550
1.0	3.0	1.0	0.87200	0.87810	0.85710
1.0	3.0	10.0	0.31520	0.32560	0.30810
1.0	5.0	0.1	0.99310	1.01460	0.99170
1.0	5.0	1.0	0.92500	0.94610	0.91520
1.0	5.0	10.0	0.45360	0.48270	0.44140

0.70861, and, $\psi_{av} = 0.42304$, respectively. Here, the maximum deviation $|\psi - \psi_{av}|/\psi_{av}$ for all τ_L is less than 0.0037%. However, the maximum deviation is up to 0.3% in Ref. [16] for MLPG method using 9 nodes.

The averaged dimensionless radiative heat fluxes in the case of blackbody boundaries and linear refractive index are shown in Table 2 for various combination of n_0, n_L and τ_L. Those results by ray tracing (RT) and by MLPG are copied from Refs. [13,16] for comparison. From Table 2, compared with RT, the maximum relative error of the averaged dimensionless radiative heat flux by MLPG [16], computed by $|\psi_{MLPG} - \psi_{RT}|/\Psi_{RT}$, is 6.415%. However the same comparative values computed by $|\psi_{SP\text{-}DOM} - \psi_{RT}|/\Psi_{RT}$ in the present work is less than 2.7%.

4.2. Example 2: Radiative equilibrium in non-scattering media with sinusoidal refractive index

Similar as in Refs. [8,17], in this case, a non-linear refractive index is adopted. The temperatures of boundary walls are assumed as $T_0 = 1000$ K and $T_L = 1500$ K, respectively. The absorption coefficient k_a and scattering coefficient k_s are uniform through the slab. The refractive index of media within the slab has a sinusoidal change along the axis coordinate as $n(x) = 1.8 - 0.6\sin(\pi x/L)$. The media within the slab is non-scattering and the optical thickness is $\tau_L = 1.0$.

Fig. 3 shows the temperature distributions by SP-DOM within the slab for two different wall emissivities, namely, $\varepsilon_0 = \varepsilon_L = 0.7$ and $\varepsilon_0 = \varepsilon_L = 1.0$. The CPU time are 1.2312, 0.7943 s for $\varepsilon_0 = \varepsilon_L = 0.7$ and $\varepsilon_0 = \varepsilon_L = 1.0$, respectively, when using $N_{node} = 9$ and $M = 8$. As shown in Fig. 3, the results by SP-DOM agree well with those by pseudo source adding method [8] and those by LSSEM [17]. The maximum relative error of our results is less than 0.6% compared with the values of Ref. [8].

Fig. 4 shows the effects of various combinations of nodes and angular directions on numerical results under the case of $n(x) = 1.8 - 0.6\sin(\pi x/L)$, $\tau_L = 1.0$, and $\varepsilon_0 = \varepsilon_L = 1.0$. Clearly, the combination of $N_{node} = 5$ and $M = 4$ almost gives the same smooth curves as the combination of $N_{node} = 99$ and $M = 12$ does. The convergent characteristic of SP-DOM is demonstrated again in this article.

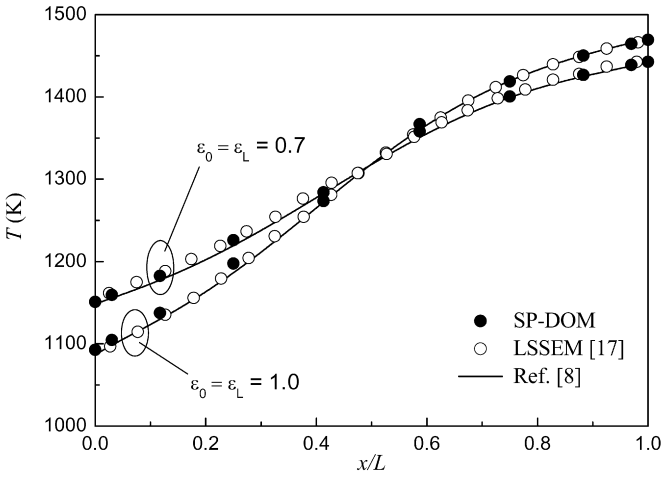

Fig. 3. Temperature distributions in the case of $n(x) = 1.8 - 0.6\sin(\pi x/L)$, $\tau_L = 1$.

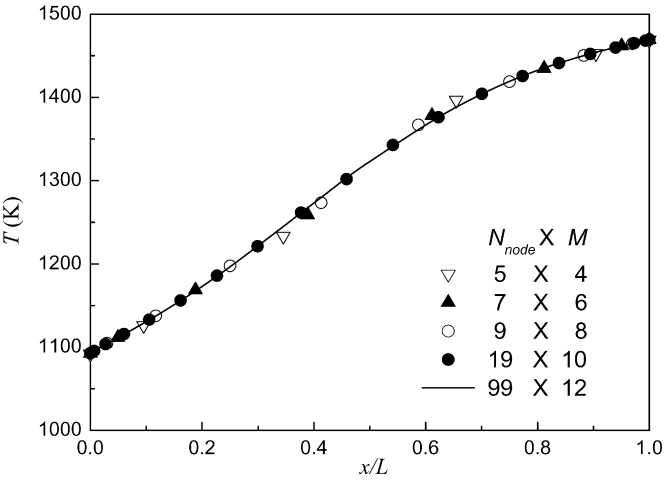

Fig. 4. Effects of various combinations of nodes and angular directions on the numerical predictions in the case of $n(x) = 1.8 - 0.6\sin(\pi x/L)$, $\tau_L = 1$ and $\varepsilon_0 = \varepsilon_L = 1.0$.

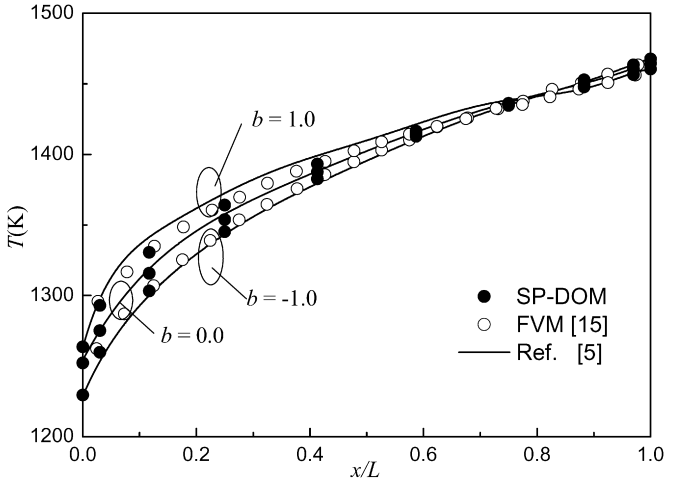

Fig. 5. Temperature distributions in the cases of $n(x) = 1.2 + 0.6x/L$, $\varepsilon_0 = \varepsilon_L = 1.0$, $\tau_L = 1$ and $\omega = 0.8$.

4.3. Example 3: Radiative equilibrium in space independent scattering media with linear refractive index

We consider one-dimensional slab filled with scattering gray media. The single scattering albedo of media is $\omega = 0.8$, and the single scattering phase function is assumed to be linear as $\Phi = 1 + b\mu\mu'$. The slab is bounded by black walls and the slab optical thickness is $\tau_L = 1.0$. The temperatures of boundary walls are assumed to be $T_0 = 1000$ K and $T_L = 1500$ K, respectively. The absorption coefficient and the scattering coefficient are uniform through the slab, but the refractive index of media is a linear function of spatial coordinate x as $n(x) = 1.2 + 0.6x/L$.

The temperature distributions by SP-DOM within the slab are shown in Fig. 5 for three values of asymmetry factor b, namely, -1, 0 and 1. For the purpose of comparisons, the predictions by Monte Carlo curved ray-tracing method [5] and finite volume method [15] are simultaneously presented in Fig. 5. The SP-DOM results agree with those of Monte Carlo curved ray-tracing method and FVM very well, and the maximum relative error referred to the predictions of Ref. [5] is less than 0.95%. For SP-DOM, the CPU time are 2.0118, 2.5473, and 0.6731 s corresponding to three values of asymmetry factor, i.e., $b = -1$, $b = 0$ and $b = 1$, when using $N_{\text{node}} = 9$ and $M = 8$, respectively.

4.4. Example 4: Radiative equilibrium in space dependent scattering media with linear refractive index

From practical significance, more complicated situations may appear such as anisotropic and space dependent scattering. In order to examine the flexibility of SP-DOM for more complicated problems, we finally used one-dimensional radiative heat transfer example with graded index and space dependent scattering media. The governing equation for such problem based on discrete ordinates method is referred to Eq. (5) on the domain of $[0, 1] \times [-1, 1]$, but the space dependent scattering coefficient k_s should be replaced by $k_s(x)$ and the source term is switched to zero. Same as in Ref. [29], keep the extinction coefficient a unit value, i.e., $\beta(x) = k_a(x) + k_s(x) = 1$. The scattering phase function is defined by

$$\Phi = \sum_{l=0}^{L} d_l P_l(\mu) P_l(\mu'), \quad d_0 = 1 \tag{19}$$

where $P_l(\mu)$ are Legendre polynomials and d_l are specified corresponding coefficients, and $L = 0$ corresponds to isotropic scattering. In this case, we choose $L = 7$ and $d_l = \{1.0, 1.98398, 1.50823, 0.70075, 0.23489, 0.05133, 0.00760, 0.00048\}$.

The expressions of boundary conditions are

$$I(0, \mu) = 1 \quad \text{on } x = 0,\ \mu \in (0, 1] \tag{20a}$$

$$I(1, \mu) = 0 \quad \text{on } x = 1,\ \mu \in [-1, 0) \tag{20b}$$

This case within uniform index media has also been used as a test case by Pontaza et al. [29].

For different graded indexes, say, $n = 1.0$, $n(x) = 1.0 + 0.1x/L$, and $n(x) = 1.0 + 0.3x/L$, the computed radiative intensity by SP-DOM with $N_{\text{node}} = 9$ and $M = 8$ is plotted in color contour lines in Fig. 6.

As shown in Fig. 6, the refractive index gradient can significantly affect the radiative intensity distributions. Compared to Fig. 6(a) with $n = 1.0$, the radiative intensities in the whole domain shown in Fig. 6(b) increased very clearly with the increasing of refractive index gradient from $n = 1.0$ up to $n(x) = 1.0 + 0.1x/L$. Increase with the refractive index gradient from $n(x) = 1.0 + 0.1x/L$ (corresponding to Fig. 6(b)) up to $n(x) = 1.0 + 0.3x/L$ (corresponding to Fig. 6(c)), the radiative intensity is intensified obviously.

In graded index media, the ray goes along a curved trajectory determined by the Fermat principle. According to Fig. 1 in Ref. [2], some possible trajectories passing through a given internal point, for given angular directions of propagation; the trajectory passing through z^* is a particular trajectory which is totally back reflected towards the left interface and cannot reach the right interface. So, the radiative intensities in the whole domain increased in graded index media as shown in Fig. 6 in present work.

5. Conclusions

To avoid the complicated computation of curved ray tracing, the Chebyshev collocation spectral method based on discrete ordinates equation is successfully applied to solve radiative heat transfer problem in semitransparent graded index media. The spatial dependent radiative intensity is expressed by Chebyshev polynomials, and the governing equations are discretized using Chebyshev collocation points in space. The results of the SP-DOM formulation are compared with those available data in the literatures for variable refractive index. The comparisons indicate that the SP-DOM has a good accuracy and efficiency even using only 9 nodes and 8 angular directions. Effects of refractive index gradient on radiative intensity distributions are also studied.

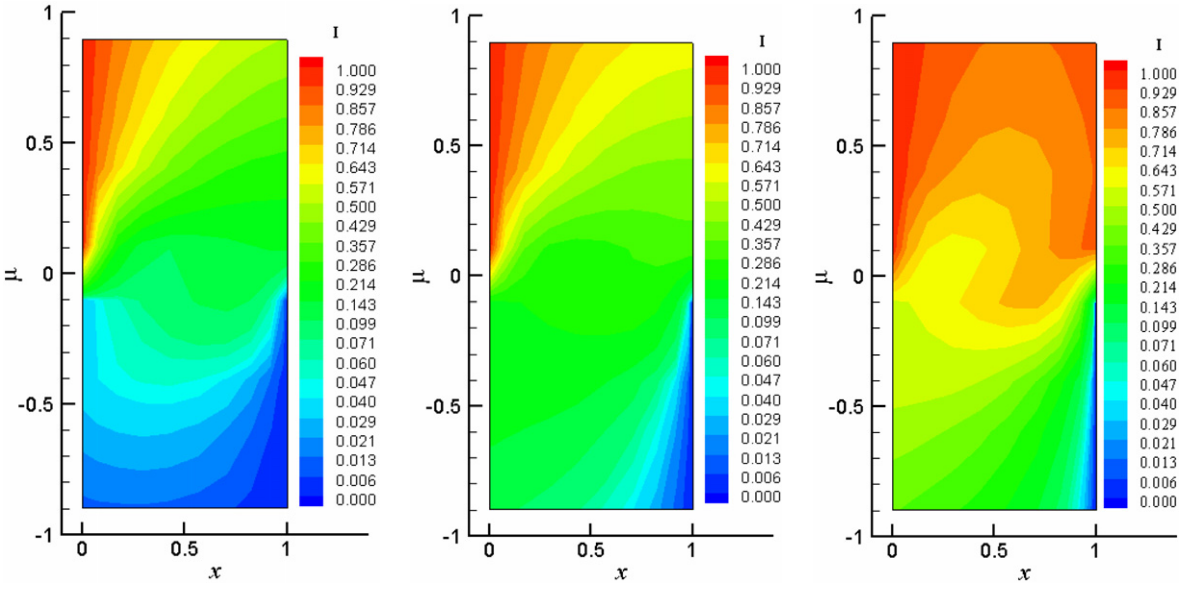

Fig. 6. Effects of refractive index gradient on the radiative intensity distribution. (a) $n = 1.0$, (b) $n(x) = 1.0 + 0.1x/L$, (c) $n(x) = 1.0 + 0.3x/L$.

Acknowledgement

This work was supported by the National Fundamental Research Programme of China (No. 2006CB601203).

References

[1] R. Siegel, C.M. Spuckler, Variable refractive index effects on radiation in semitransparent scattering multilayered regions, Journal of Thermophysics and Heat Transfer 7 (4) (1993) 624–630.
[2] P. Ben Abdallah, V. Le Dez, Temperature field inside an absorbing-emitting semitransparent slab at radiative equilibrium with variable spatial refractive index, Journal of Quantitative Spectroscopy and Radiative Transfer 65 (4) (2000) 595–608.
[3] P. Ben Abdallah, V. Le Dez, Thermal emission of a semi-transparent slab with variable spatial refractive index, Journal of Quantitative Spectroscopy and Radiative Transfer 67 (3) (2000) 185–198.
[4] Y. Huang, H.P. Tan, X.L. Xia, Apparent emitting characteristics of semi-transparent isothermal medium layer with graded index, Journal of Infrared and Millimeter Waves 20 (5) (2001) 348–352 (in Chinese).
[5] L.H. Liu, H.P. Tan, Q.Z. Yu, Temperature distributions in an absorbing-emitting-scattering semitransparent slab with variable spatial refractive index, International Journal of Heat and Mass Transfer 46 (15) (2003) 2917–2920.
[6] Y. Huang, X.L. Xia, H.P. Tan, Temperature field of radiative equilibrium in a semitransparent slab with a linear refractive index and gray walls, Journal of Quantitative Spectroscopy and Radiative Transfer 74 (2) (2002) 249–261.
[7] Y. Huang, X.L. Xia, H.P. Tan, Radiation equilibrium temperature field in a gradient index medium with specular surfaces, Heat and Mass Transfer 39 (10) (2003) 835–842.
[8] Y. Huang, X.L. Xia, H.P. Tan, Comparison of two methods for solving radiative heat transfer in a gradient index semitransparent slab, Numerical Heat Transfer: Part B—Fundamentals 44 (1) (2003) 83–99.
[9] H.P. Tan, Y. Huang, X.L. Xia, Solution of radiative heat transfer in a semi-transparent slab with an arbitrary refractive index distribution and diffuse gray boundaries, International Journal of Heat and Mass Transfer 46 (11) (2003) 2005–2014.
[10] Y. Huang, X.L. Xia, H.P. Tan, Coupled radiation and conduction in a graded index layer with specular surfaces, Journal of Thermophysics and Heat Transfer 18 (2) (2004) 281–285.
[11] H.P. Tan, H.L. Yi, J.F. Luo, H.C. Zhang, Transient coupled heat transfer inside a scattering medium with graded refractive index, Journal of Thermophysics and Heat Transfer 20 (3) (2006) 583–594.
[12] Y. Huang, X.G. Liang, Approximate thermal emission models of a two-dimensional graded index semitransparent medium, Journal of Thermophysics and Heat Transfer 20 (1) (2006) 52–58.
[13] D. Lemonnier, V. Le Dez, Discrete ordinates solution of radiative transfer across a slab with variable refractive index, Journal of Quantitative Spectroscopy and Radiative Transfer 73 (2–5) (2002) 195–204.
[14] L.H. Liu, Finite element solution of radiative transfer across a slab with variable spatial refractive index, International Journal of Heat and Mass Transfer 48 (11) (2005) 2260–2265.
[15] L.H. Liu, Finite volume method for radiation heat transfer in graded index medium, Journal of Thermophysics and Heat Transfer 20 (1) (2006) 59–66.
[16] L.H. Liu, Meshless method for radiative heat transfer in graded index medium, International Journal of Heat and Mass Transfer 49 (1–2) (2006) 219–229.
[17] J.M. Zhao, L.H. Liu, Solution of radiative heat transfer in graded index media by least square spectral element method, International Journal of Heat and Mass Transfer 50 (13–14) (2007) 2634–2642.
[18] D. Gottlieb, S.A. Orszag, Numerical analysis of spectral methods: Theory and applications, in: Regional Conference Series in Applied Mathematics, vol. 28, SIAM, Philadelphia, 1977, pp. 1–168.
[19] C. Canuto, M.Y. Hussaini, A. Quarteroni, T.A. Zang, Spectral Methods in Fluid Dynamics, Springer-Verlag, New York, 1988.
[20] R. Peyret, Spectral Methods for Incompressible Viscous Flow, Springer-Verlag, New York, 2002.
[21] F.B. Belgacem, M. Grundmann, Approximation of the wave and electromagnetic diffusion equations by spectral methods, SIAM Journal on Scientific Computing 20 (1) (1998) 13–32.
[22] X.W. Shan, D. Montgomery, H.D. Chen, Nonlinear magnetohydrodynamics by Galerkin-method computation, Physical Review A 44 (10) (1991) 6800–6818.
[23] X.W. Shan, Magnetohydrodynamic stabilization through rotation, Physical Review Letters 73 (12) (1994) 1624–1627.
[24] N. Aouled-Dlala, T. Sghaier, E. Seddiki, Numerical solution of radiative and conductive heat transfer in concentric spherical and cylindrical media, Journal of Quantitative Spectroscopy and Radiative Transfer 107 (3) (2007) 443–457.
[25] B.W. Li, Y.S. Sun, Y. Yu, Iterative and direct Chebyshev collocation spectral methods for one-dimensional radiative heat transfer, Interna-

tional Journal of Heat and Mass Transfer (2008), in press, doi:10.1016/j.ijheatmasstransfer.2008.04.048.
[26] M.F. Modest, Radiative Heat Transfer, second ed., Academic Press, San Diego, CA, 2003.
[27] R. Siegel, J.R. Howell, Thermal Radiation Heat Transfer, fourth ed., Taylor and Francis, New York, 2002.
[28] J.P. Boyd, Chebyshev and Fourier Spectral Methods, second ed., Dover, New York, 2001.
[29] J.P. Pontaza, J.N. Reddy, Least-squares finite element formulations for one-dimensional radiative transfer, Journal of Quantitative Spectroscopy and Radiative Transfer 95 (3) (2005) 387–406.